An Experimental Study on a Dual Stator Winding-Mixed Pole-Brushless Generator with Different Rotors and Different Excitations

M Ezzat, M El_Shanawany and SMR Tahoun
Faculty of Engineering
Minoufiya University
Egypt

***Abstract*–This paper presents an experimental study to show the performance of a dual stator winding mixed pole brushless generator with different rotor types and different excitations. In this paper, the performance is measured with salient pole, flux barrier and cage rotors. The study results in two new generator types named; a mixed pole synchronous generator and a constant frequency generator.**

Keywords– Brushless, Dual Stator Winding, Experimental Study, Mixed Pole.

I. INTRODUCTION

Recently, the interest on dual winding mixed pole brushless machines has been increased in attempts from researchers to increase the electrical machines reliability and to reduce the need for maintenance. Brushless doubly-fed induction machine (BDFIM) and brushless doubly-fed reluctance machine (BDFRM) are two examples of such machines that found a great interest and study in a lot of literatures [1-15]. According to [16], slight modifications on the BDFRM results in a new machine called a dual stator winding-mixed pole-brushless synchronous generator (DSW-MBSG). This paper presents an experimental study on the dual stator winding-mixed pole machine with three rotor types named; salient pole, flux barrier and squirrel cage rotors. The study results in two new different machines that can be improved and used in the future.

II. DUAL STATOR WINDING MIXED POLE GENERATOR CONSTRUCTION

The studied generator consists of stator and rotor. The stator is of silicon steel laminations. There are slots in its internal periphery. The stator is wound with two three- phase winding sets with different pole number. In this paper the stator of a 1 hp conventional ac induction machine has been used after rewinding it with two three-phase sets. One of the two sets is wound with 2-pole and the other with 6-pole. Fig. 1 shows the photo of the experimental stator. In this paper, the rotor of the studied generator comes in three shapes they are: a 4-pole salient rotor, a 4-pole flux barrier rotor and a cage rotor. Fig. 2 shows the photos of these rotors.

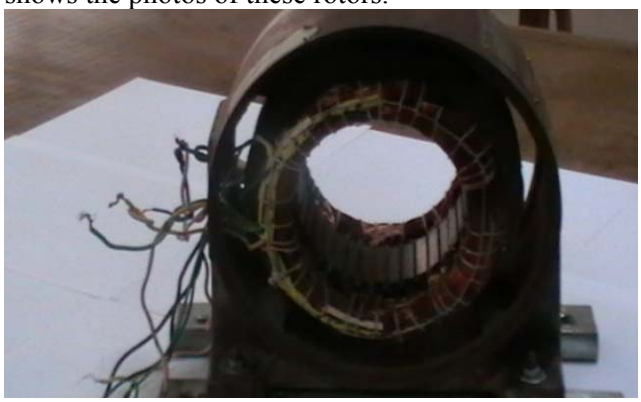

Experimental Stator of the Dual Stator Winding Mixed Pole Machine

Fig. 1

Salient Pole and Flux Barrier Rotors

Fig. 2a

Squirrel Cage Rotor

Fig. 2b

III. MIXED POLE MACHINE AS A SYNCHRONOUS GENERATOR

The dual stator winding-mixed pole-brushless machine can be operated as a synchronous generator. This can be done be connecting the 6-pole winding as open delta with two reversed phases as shown in Fig. 3. The reconnected winding is supplied from a dc source. The resultant field links the generation winding (2-pole winding) through the rotor. As the field is non time varying, the rotor must be a reluctance type rotor.

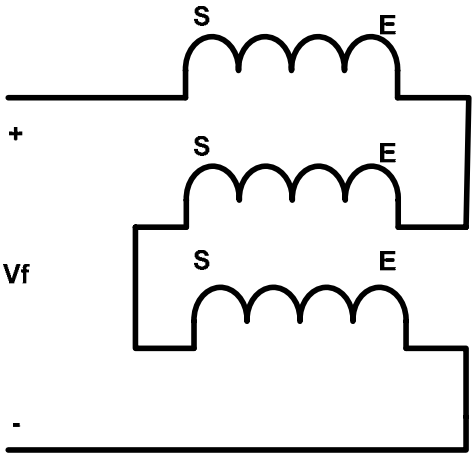

Open Delta with Two Reversed Phases for Field Connection

Fig. 3

Voltage equations for the mixed pole synchronous generator can be written as follows:

$V_f = r_f i_f + p\lambda_f$ (1)

$V_{Gabc} = -r_G i_{Gabc} + p\lambda_G$ (2)

Where:

*i_f: is the field winding current (DC current).
*i_{Gabc}: is the generating winding current (AC current).
*r_f: is the field winding resistance.
*r_G: is the generating winding resistance per phase.
*V_f: is the applied field voltage (DC voltage).
*V_{Gabc}: is the generating winding terminal voltage (AC voltage).
*λ_f: is the flux linking field winding.
*λ_G: is the flux linking generating winding phases.

To calculate the flux linkage, machine inductances must be calculated. The technique adopted here is the winding function analysis (WFA) technique to take the effect of space harmonics into account. Inductances are calculated using the following formula:

$$L_{ij}(\theta_{rm}) = \mu_0 rl \int_0^{2\pi} g^{-1}(\theta_{rm}, \Phi) N_i(\theta_{rm}, \Phi) N_j(\theta_{rm}, \Phi) d\Phi \quad (3)$$

Figs.4 & 5 show the winding functions for a one phase of the 6-pole winding and a one phase of the 2-pole winding respectively.

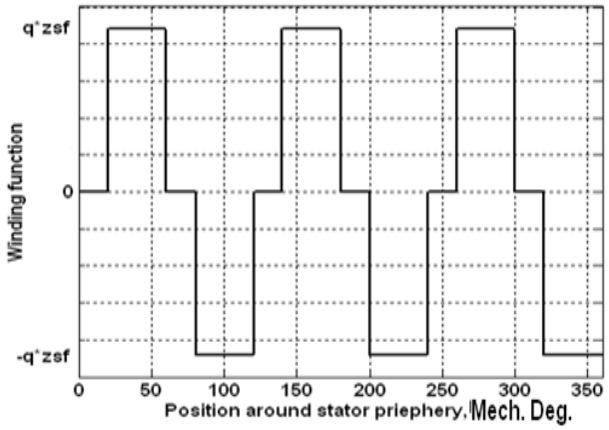

Winding function of a 6-pole winding phase

Fig. (4)

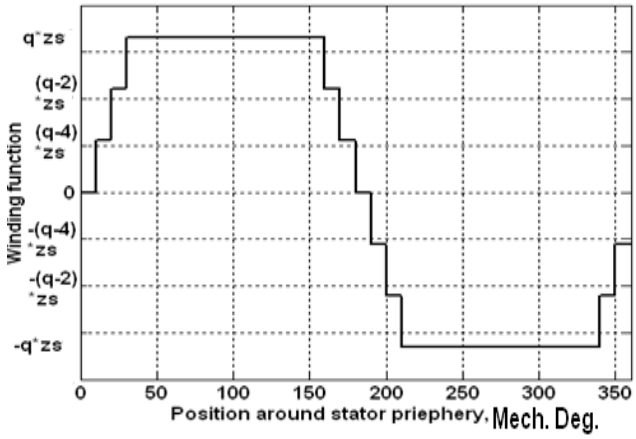

Winding function of a 2-pole winding phase

Fig. (5)

Where:

q: is the slot per pole per phase divided by two.
z_{sf}: is the number of field conductors per slot.
Z_s: is the number of generation conductors per slot.

Figs 6 & 7 show the inverse air gap function (g^{-1}) adopted for salient pole and flux barrier rotors respectively. One can see that effect of slotting is taken into account for both air gap models.

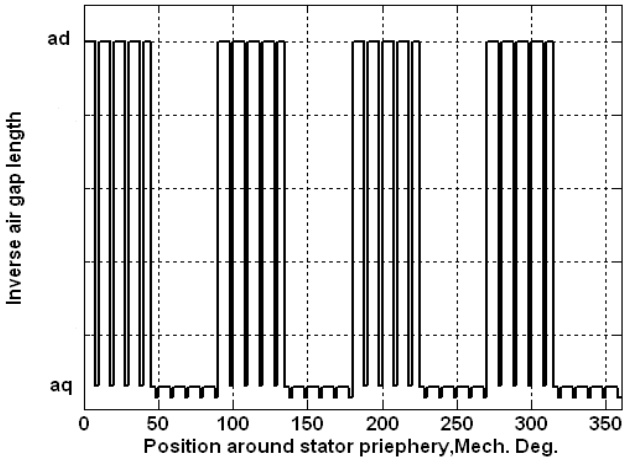

Inverse air gap function for salient pole rotor

Fig. 6

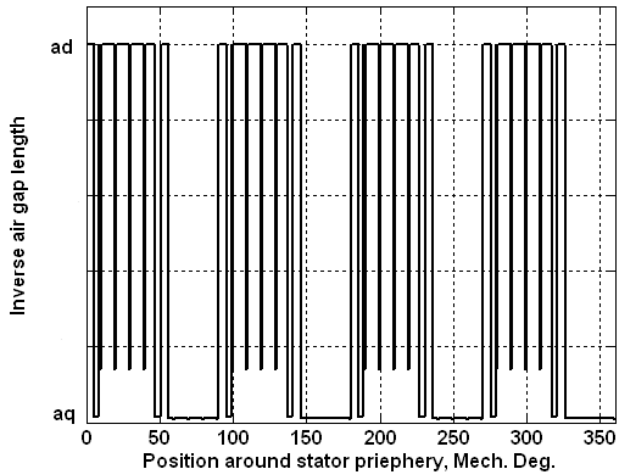

Inverse air gap function for flux barrier rotor
Fig. 7

Where:
ad: is the inverse air gap function in the d-axis.
aq: is the inverse air gap function in the q-axis.

Based on equation (3), machine inductances can be calculated using a MATLAB M-FILE. Figs. 8 to 11show a sample of the calculated machine inductances.

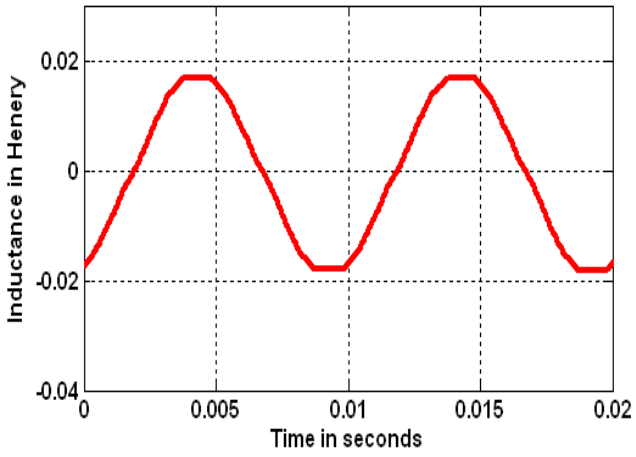

Mutual inductance with salient pole rotor
Fig. 8

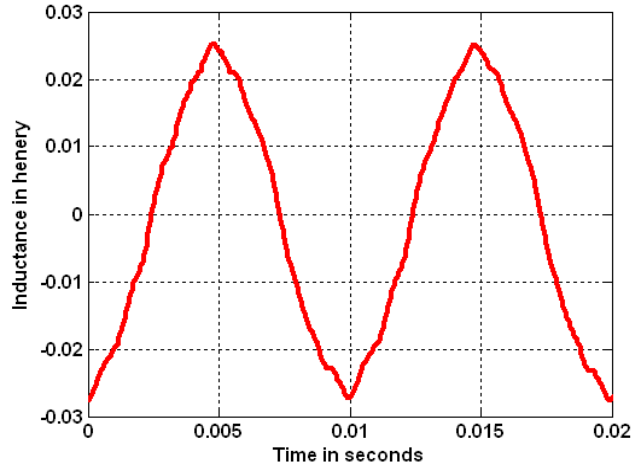

Mutual inductance with flux barrier rotor
Fig. 9

From the above figures, it can be seen that mutual inductance obtained with the flux barrier rotor is higher than the obtained value with the salient pole one. So that it is expected that more voltage will be generated with the flux barrier rotor than the salient pole one.

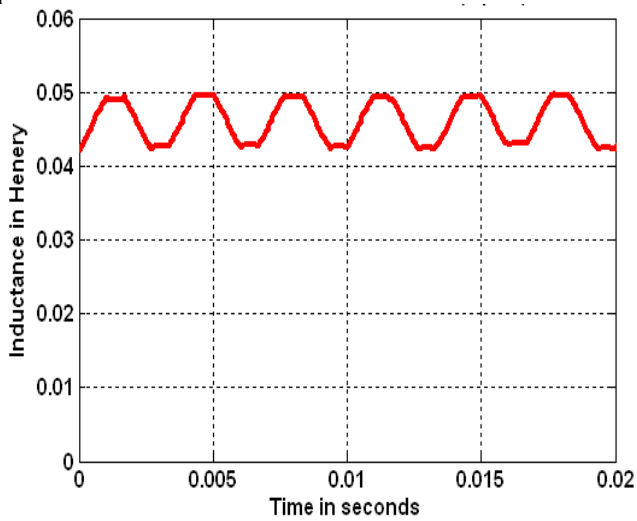

Self inductance of a 6-pole phase with the salient pole rotor
Fig. 10

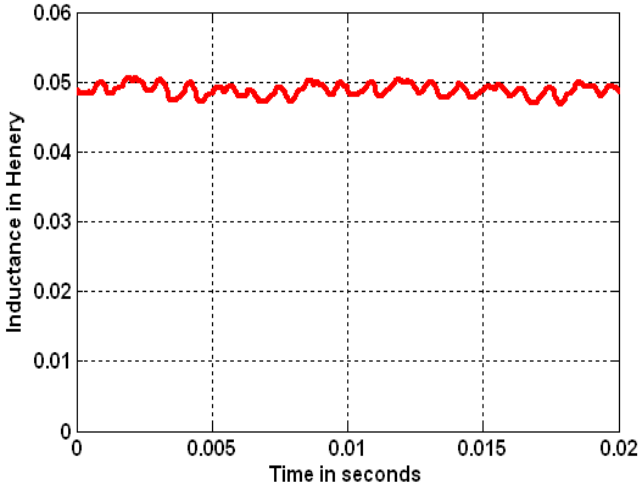

Self inductance of a 6-pole phase with the flux barrier rotor
Fig. 11

One can see that self inductances either of 6-pole or 2-pole windings are not purely constant but they have AC components.
From equations (1&2) and the calculated inductances a MATLAB SIMULINK model is built to compare the obtained results with the experimental ones. Figs. 12 & 13 show the generated voltage at no_load with the salient pole and flux barrier rotors respectively. From these figures, one can see that the generated voltage with the barrier rotor is higher than it with the salient pole rotor. Also, it can be seen that the frequency is double the frequency obtained from the conventional synchronous generator of the same rotor poles.

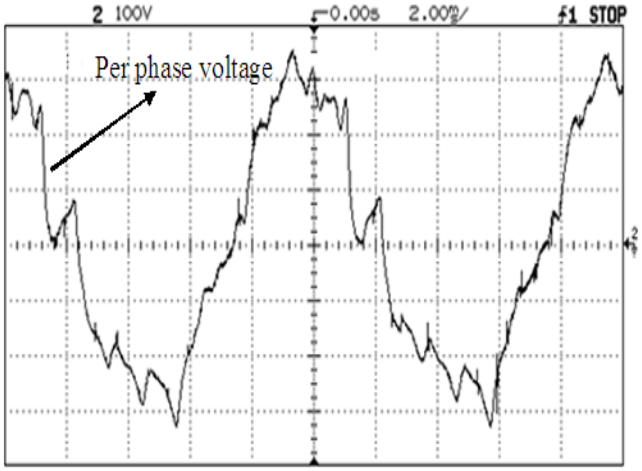

Experimental no load per phase voltage
(1500r.p.m,I_F=2A,I_L=0A, Salient pole rotor)
Voltage scale=10:1
Fig. 12a

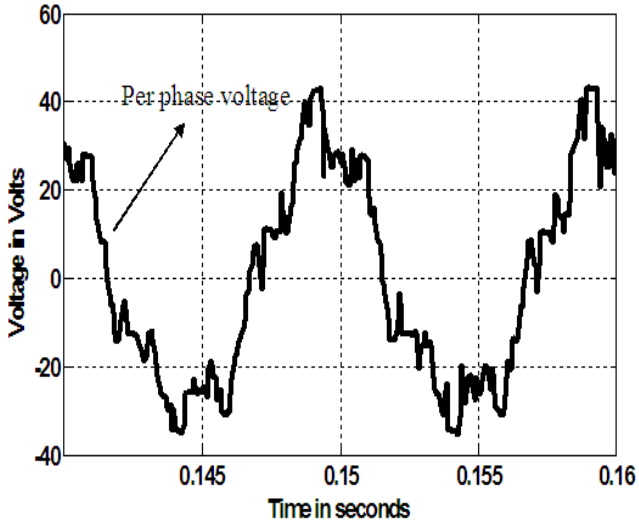

Simulated no load per phase voltage
(1500r.p.m,I_F=2A,I_L=0A, Salient pole rotor)
Fig. 12b

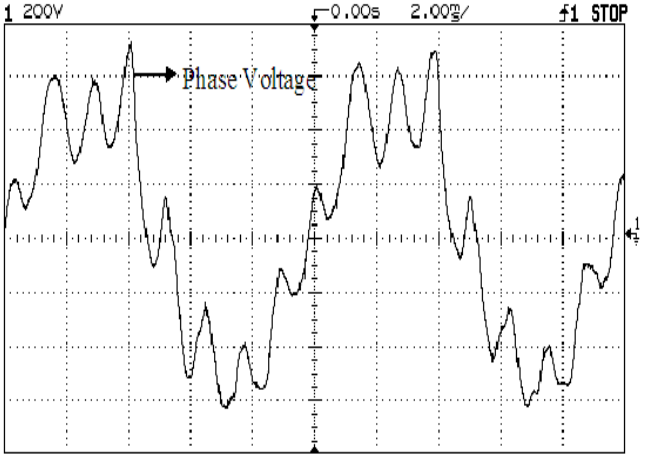

Experimental no load per phase voltage
(1500r.p.m,I_F=2A,I_L=0A, flux barrier rotor)
Voltage scale=10:1
Fig. 13a

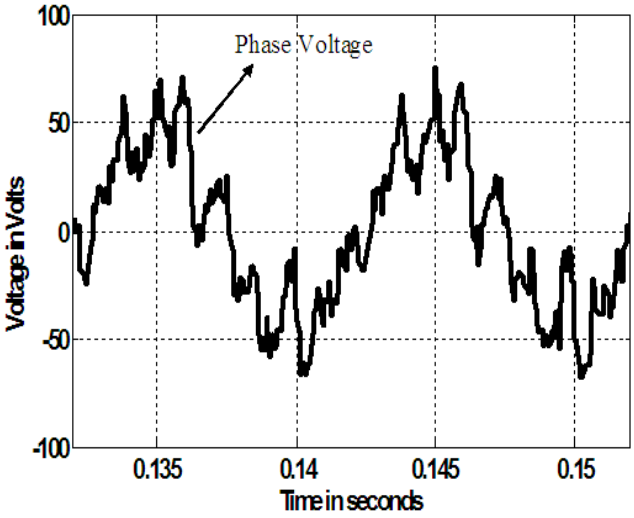

Simulated no load per phase voltage
(1500r.p.m,I_F=2A,I_L=0A, flux barrier rotor)
Fig. 13b

Figs. 14 & 15 show the terminal voltage per phase for two phases with the two rotors respectively. The important notice here is the close of the voltage waveform from the sinusoidal waveform.

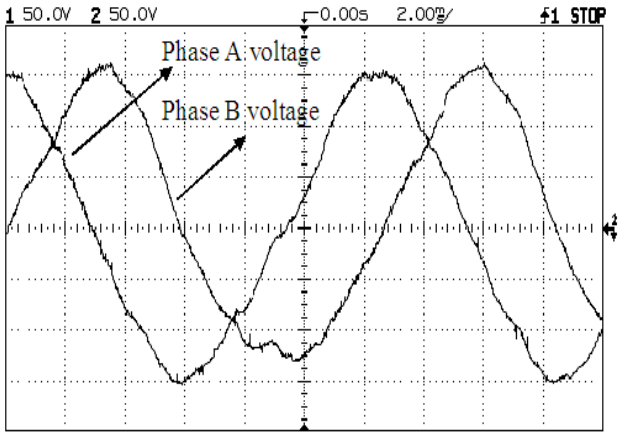

Experimental terminal voltage for phases a&b
(1500r.p.m,I_F=2A,I_L=0.55A, Salient pole rotor)
Voltage scale=10:1
Fig. 14a

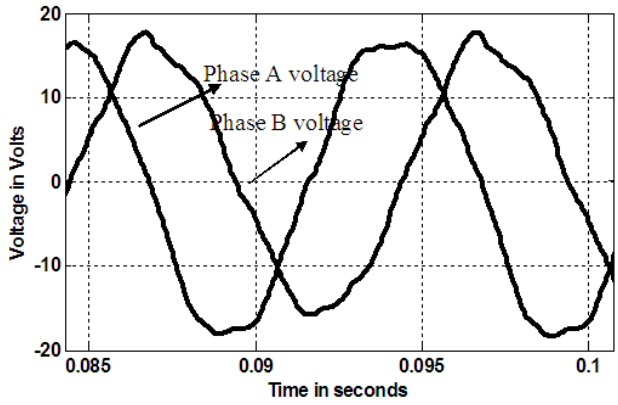

Simulated terminal voltage for phases a&b
(1500r.p.m,I_F=2A,I_L=0.55A, Salient pole rotor)
Fig. 14b

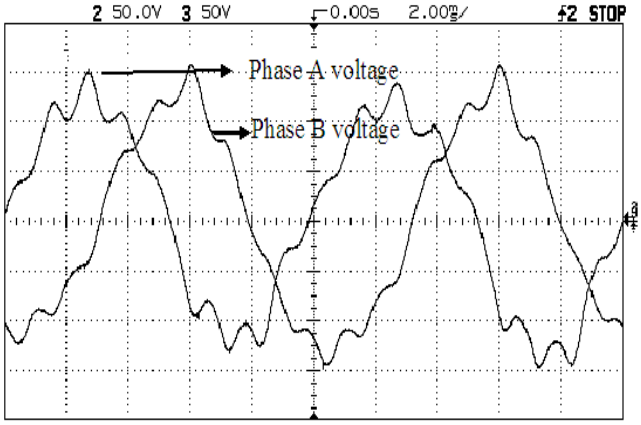

Experimental terminal voltage for phases a&b
(1500r.p.m,I_F=2A,I_L=0.9A, Flux Barrier Rotor)
Voltage scale=10:1
Fig. 15a

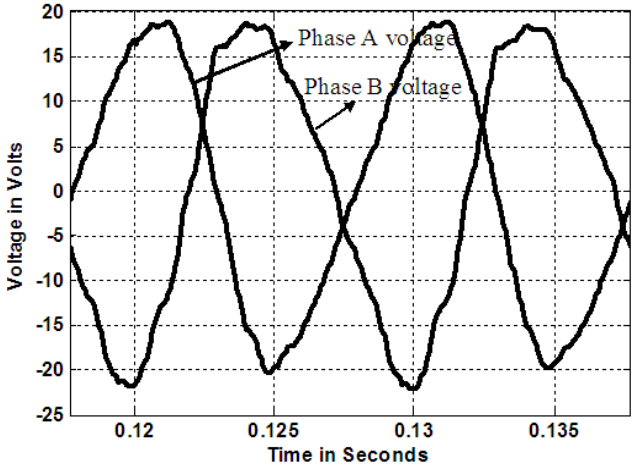

Simulated terminal voltage for phases a&b
(1500r.p.m,I_F=2A,I_L=0.9A, Flux Barrier Rotor)
Fig. 15b

Figs. 16 to 19 show the per phase voltage and current for the two reluctance rotors respectively. From these figures, one can see that the harmonic content in voltage and current waveforms is reduced especially with resistive load.

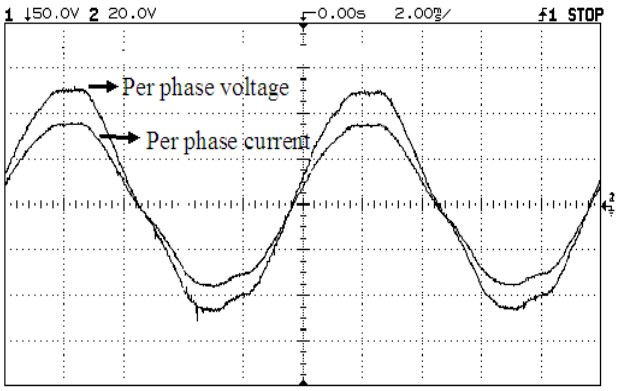

Experimental terminal voltage and phase current
(1500r.p.m,I_F=2A,I_L=0.55A, Salient pole rotor,
Resistive Load)
Voltage scale=10:1
Fig. 16a

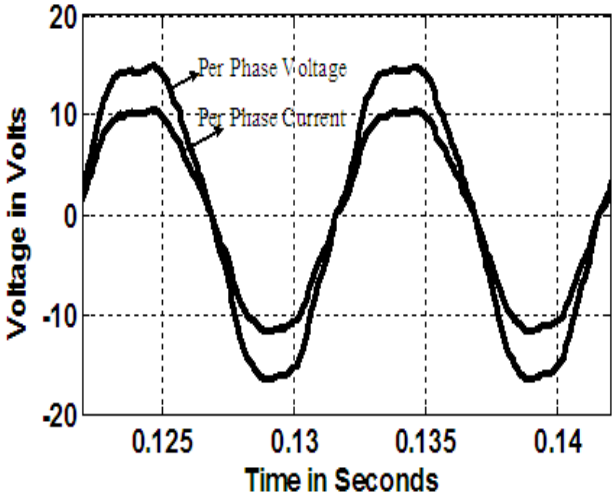

Simulated terminal voltage and phase current
(1500r.p.m,I_F=2A,I_L=0.55A, Salient pole rotor,
Resistive Load)
Fig. 16b

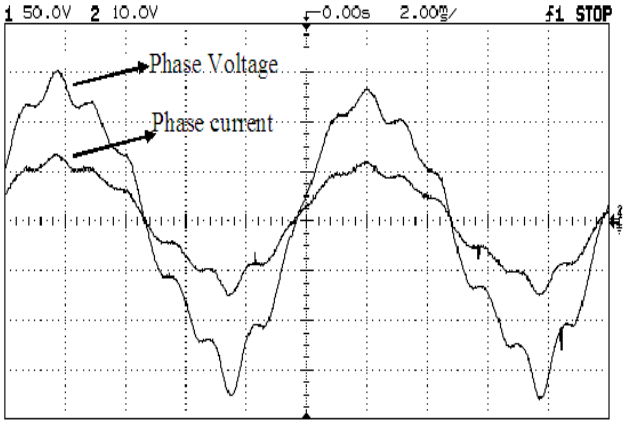

Experimental terminal voltage and phase current
(1500r.p.m,I_F=2A,I_L=0.9A, flux barrier rotor,
Resistive Load)
Voltage scale=10:1
Fig. 17a

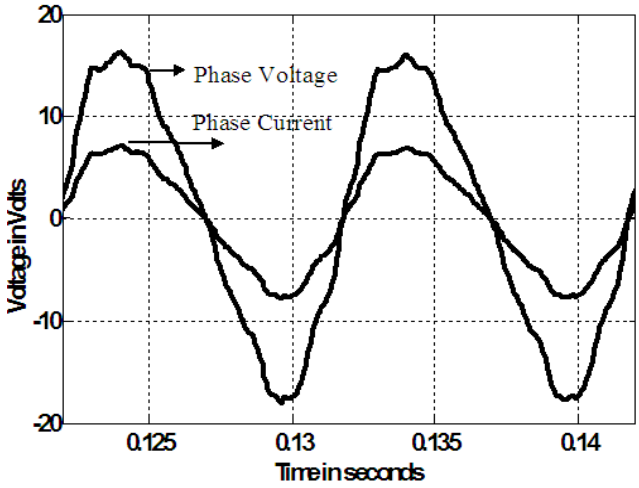

Simulated terminal voltage and phase current
(1500r.p.m,I_F=2A,I_L=0.9A, flux barrier rotor,
Resistive Load)
Fig. 17b

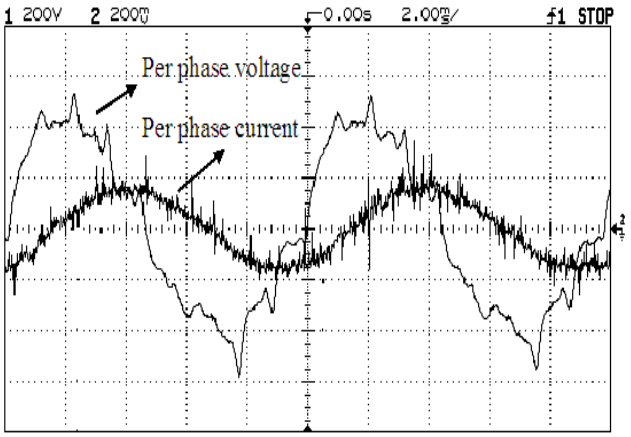

Experimental terminal voltage and phase current (1500r.p.m,I_F=2.5A,I_L=0.45A, Salient pole rotor, Inductive Load)
Voltage scale=10:1
Fig. 18a

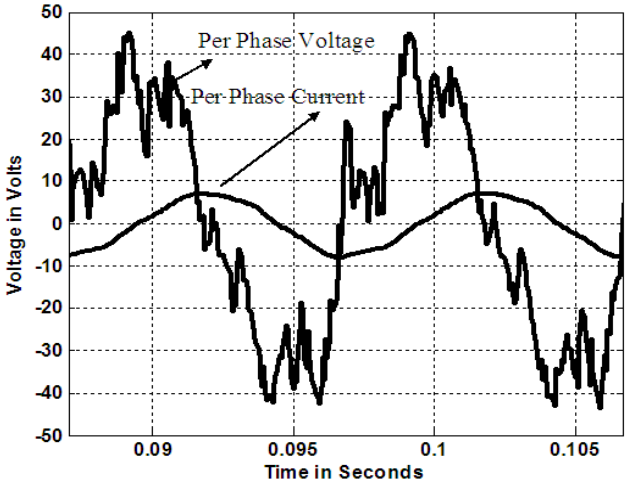

Simulated terminal voltage and phase current (1500r.p.m,I_F=2.5A,I_L=0.45A, Salient pole rotor, Inductive Load)
Fig. 18b

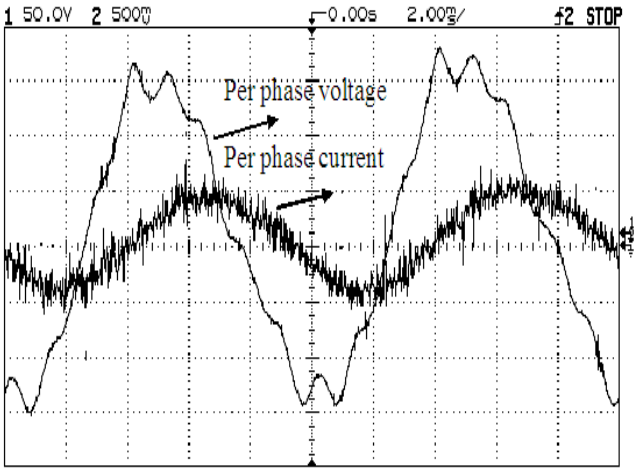

Experimental terminal voltage and phase current (1500r.p.m,I_F=2A,I_L=0.78A, Flux Barrier rotor, Inductive Load)
Voltage scale=10:1
Fig. 19a

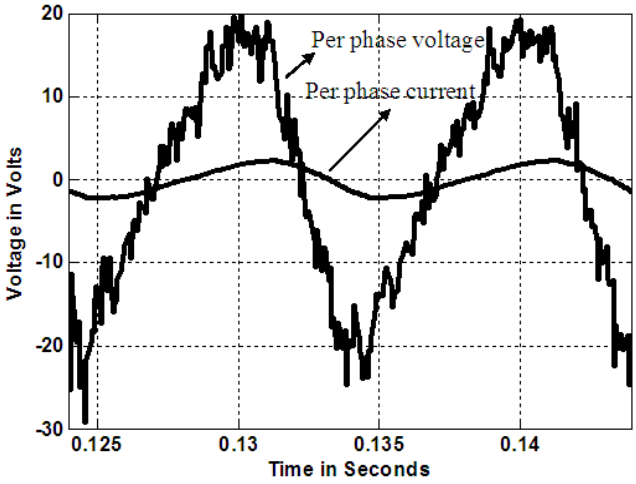

Simulated terminal voltage and phase current (1500r.p.m,I_F=2A,I_L=0.78A, Flux Barrier rotor, Inductive Load)
Fig. 19b

Figs. 20 & 21 show the field current waveform with the use of the two reluctance rotors respectively. From these figures, it can be seen that the field current contains an AC component due to the transformation to the stator side.

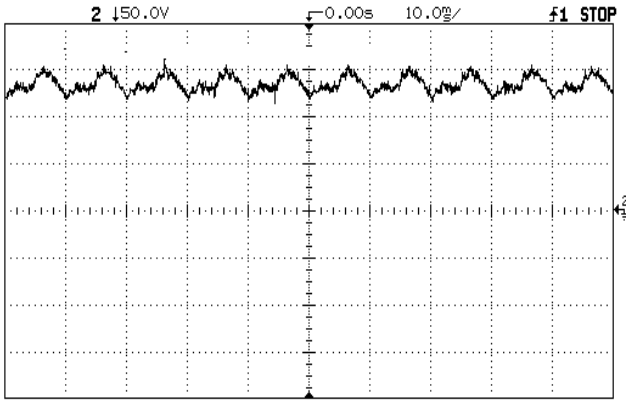

Experimental Field Current (1500r.p.m,I_F=2A, Salient pole rotor)
Fig. 20a

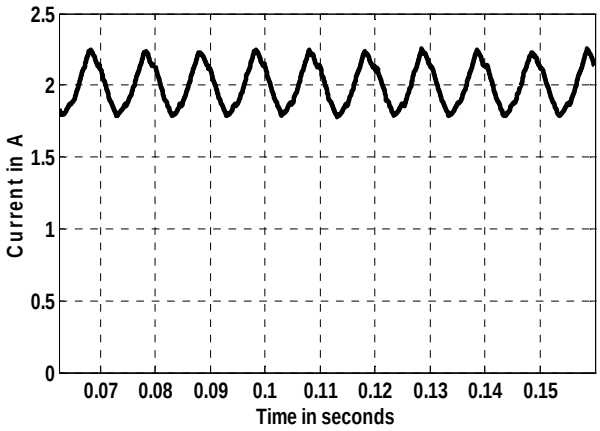

Simulated Field Current (1500r.p.m,I_F=2A, Salient pole rotor)
Fig. 20b

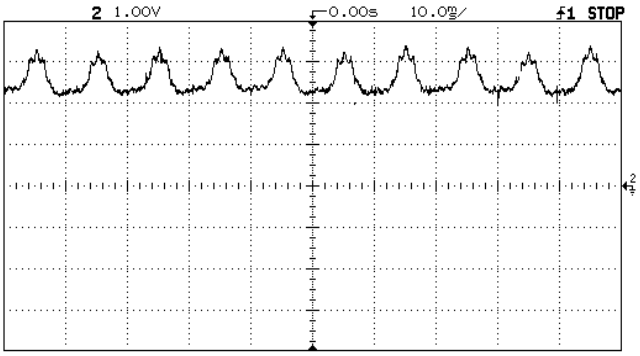

Experimental Field Current
(1500r.p.m,I_F=2A, Flux Barrier rotor)
Fig. 21a

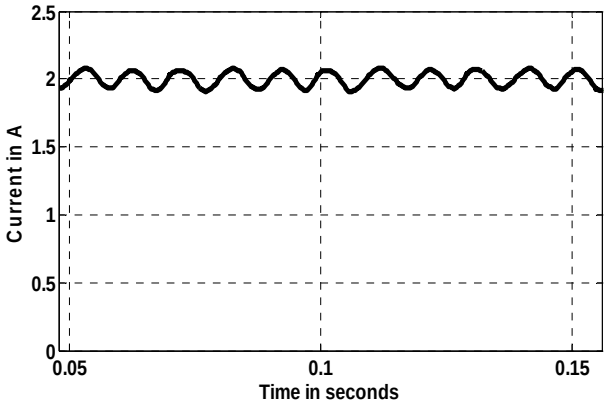

Simulated Field Current
(1500r.p.m,I_F=2A, Flux Barrier rotor)
Fig. 21b

Figs. 22 & 23 show the terminal voltage versus load current for the two reluctance rotors at two different field currents. From these figures, it can be shown that with the barrier rotor the machine power increases which means the dependency on the rotor saliency ratio.

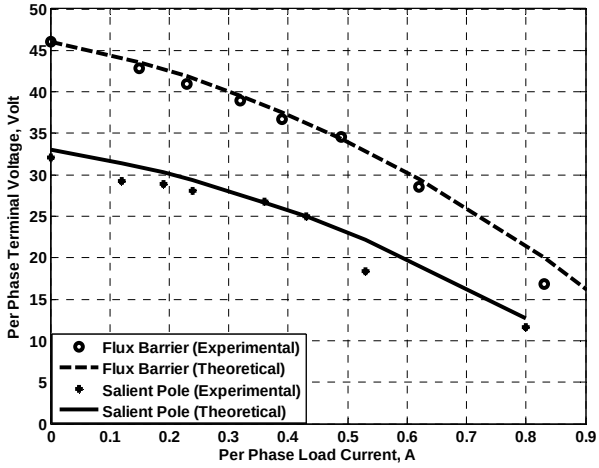

Per Phase Terminal Voltage Versus the Per Phase Load Current
(Field Current=2.5A, Rotor Speed=1500 R.P.M. , Resistive Load)
Fig. 22

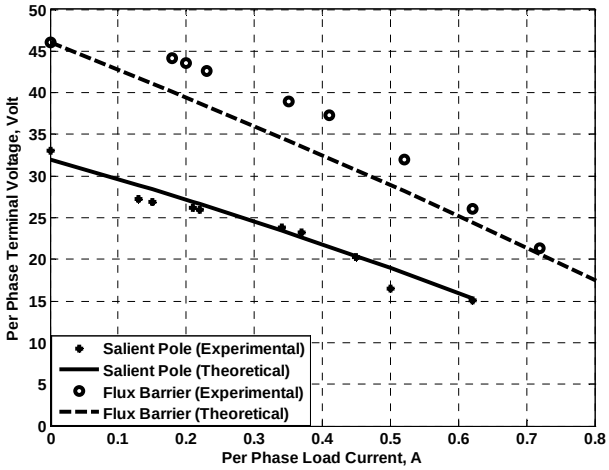

Per Phase Terminal Voltage Versus the Per Phase Load Current
(Field Current=2.5A, Rotor Speed=1500 R.P.M. ., Inductive Load)
Fig. 23

From all the above results, it can be shown that the behavior of the dual stator winding mixed pole machine with reluctance rotors is similar to the behavior of the synchronous machine with twice the rotor pole number (e.g. a mixed pole machine of 4 rotor poles is equivalent to 8-pole conventional synchronous machine).

IV. MIXED POLE MACHINE AS A CONSTANT FREQUENCY GENERATOR

To use the dual stator winding mixed pole machine as a constant frequency generator, the cage rotor can be used, the 2-pole winding must be used as a field winding by reconnecting it as open delta without phase reversal and the 6-pole winding is used as a generation winding. Another important difference here is the excitation of the field winding from a single-phase AC supply. Figs. 24a & 24b show the generated voltage per phase at different speeds and different field currents. The important notice here is the constant frequency operation with speed variation that can give this generator an advantage for the use in variable speed generation systems.

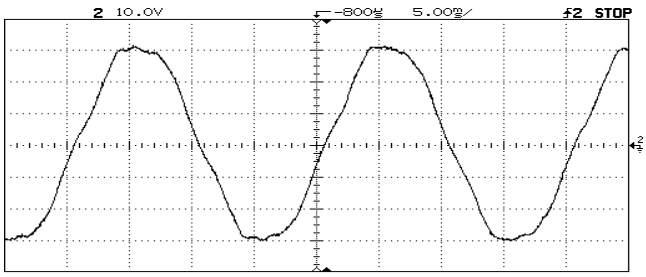

No Load Phase Voltage at Field Current=1.64A, Rotor Speed=950R.P.M.
Fig. 24a

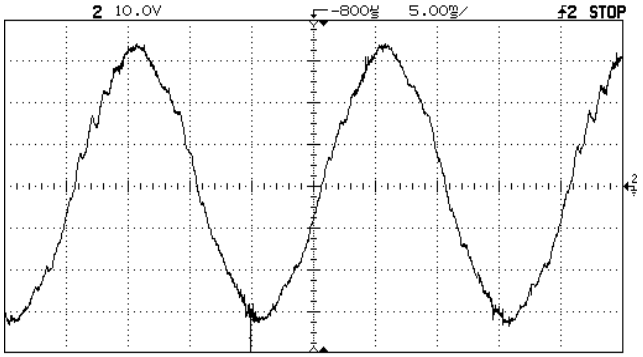

No Load Phase Voltage at Field Current=2.85A, Rotor Speed=1485R.P.M.
Fig. 24b

Figs. 25a & 25b show the waveforms of the no load line voltages at different speeds and at different field currents. It can be shown that the waveforms are very close to the sinusoidal waveform, the frequency is constant whatever the rotor speed and there is a phase shift between each line voltage of approximately 120 degree.

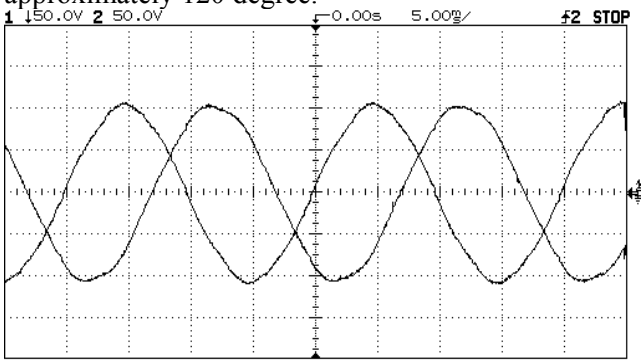

No Load Line Voltage at Field Current=1.22A, Rotor Speed=985R.P.M.
Fig. 25a

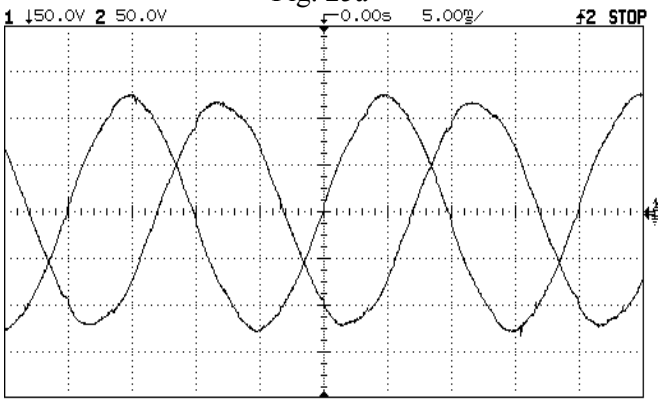

No Load Line Voltage at Field Current=1.2A, Rotor Speed=1000R.P.M.
Fig. 25b

Figs. 26a & 26b show the terminal per phase voltages for two phases at different rotor speeds, and at different field and load currents. From these figures it can be shown also the constant frequency operation whatever the rotor speed and the phase shift of approximately 120 degree in addition to the low harmonic content.

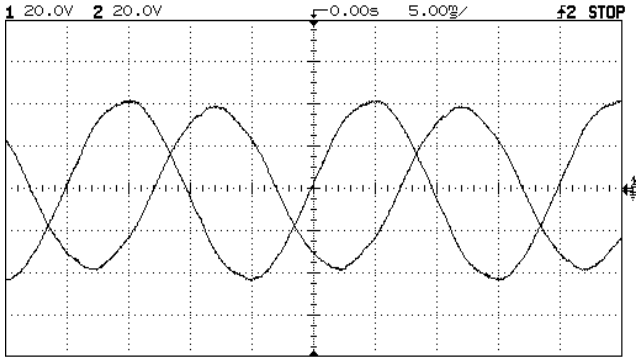

Terminal Phase Voltage at Field Current=2A, Rotor Speed=1040R.P.M.
Fig. 26a

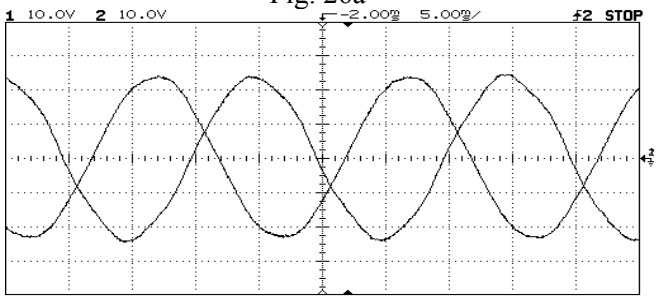

Terminal Phase Voltage at Field Current=2.56A, Rotor Speed=1280R.P.M.
Fig. 26b

Figs. 27a & 27b show the per phase terminal voltage and the per phase current for the machine loaded with resistive load and with an inductive load respectively. The voltage waveform with the resistive load is very nearer to the sine wave than the waveform with the inductive load but the frequency in the two cases is fixed at 50Hz.

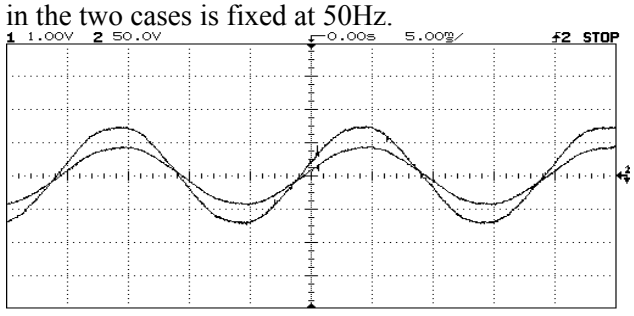

Terminal phase Voltage & Phase Current at Load Current=2.25A, Rotor Speed=1040R.P.M. & (Resistive-Load)
Fig. 27a

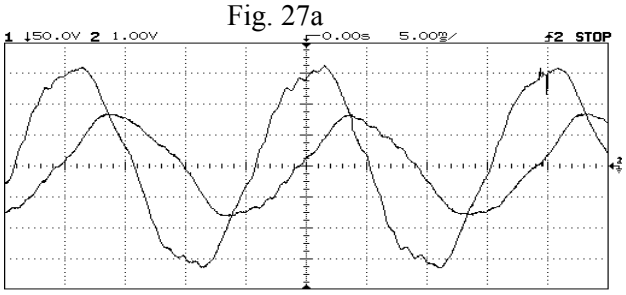

Terminal phase Voltage & Phase Current at Load Current=0.5A, Rotor Speed=1200R.P.M. & (RL-Load)
Fig. 27b

Fig. 28 shows the frequency of the terminal voltage at different rotation speeds. From this figure, it can be shown that the frequency of the generated voltage is constant at the field excitation frequency (50Hz.) whatever the rotor speed.

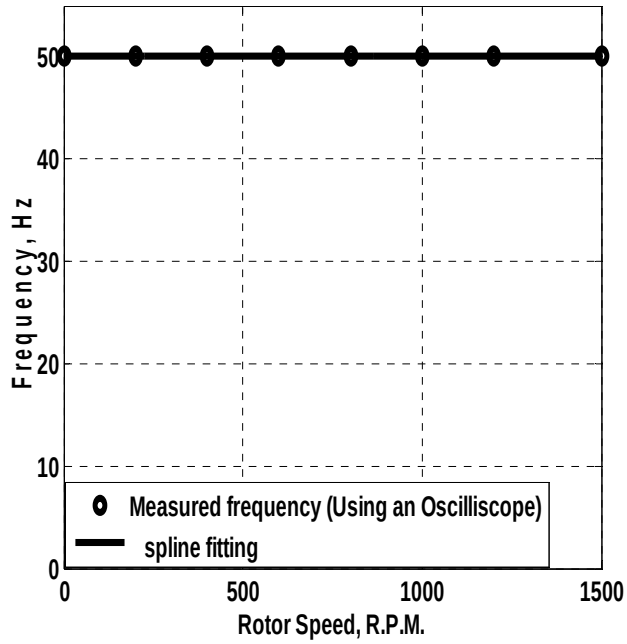

Frequency of the generated voltage versus Rotor Speed
Fig. 28

Fig. 29 shows the variation of the induced voltage versus rotor speed. It can be shown that the induced voltage is dependent on the rotor speed which means that the energy transferred to the load comes from the mechanical shaft.

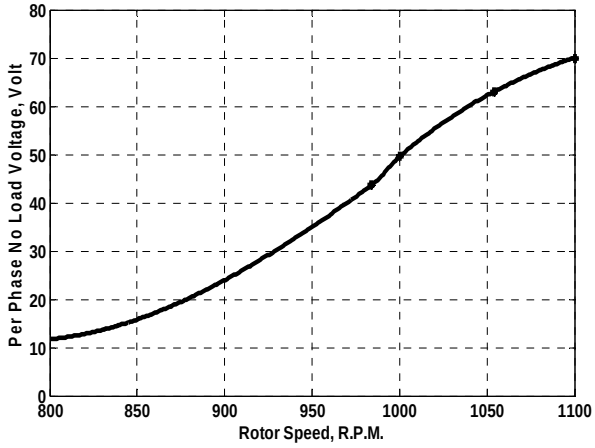

Variation of the Per Phase No Load Voltage with Rotor Speed
Fig. 29

Figs. 30a & 30b show the terminal voltage variation versus the per phase load current at different rotor speeds and at different field currents. From these figures, the voltage regulation of the machine seems to be good.

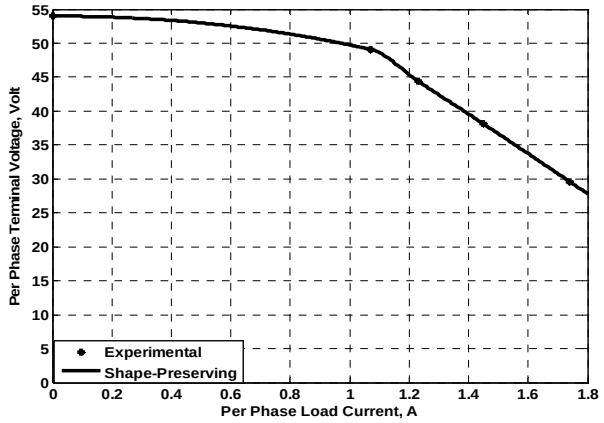

Per Phase Terminal Voltage versus the Per Phase Load Current
Field Current=2A & Rotor Speed=1000 R.P.M.
Fig. 30a

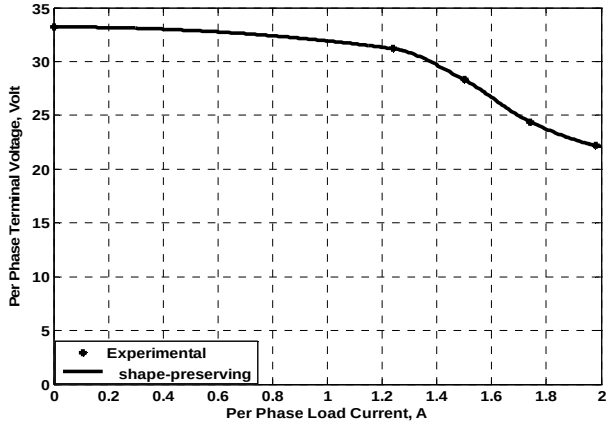

Per Phase Terminal Voltage versus the Per Phase Load Current
Field Current=1A & Rotor Speed=1030 R.P.M.
Fig. 30b

VI. CONCLUSION

An experimental study on a dual stator winding mixed pole machine has been presented. The study has shown two different generator types with the change in the machine rotor and the excitation technique. In the future, more work and experiments can be done on these machines.

REFERENCES

[1] Farhad Barati et al, *Development of a Vector Model for Brushless Doubly- Fed Machine Considering All Loops in Each Rotor Nest*,24th International Power System Conference, 2009, PP. 1-11.

[2]S. M. Allam, *Analysis and Control Characteristics of a Brushless Doubly-Fed Induction Machine*, PHD Thesis, Tanta University, 2009.

[3]Zhongchao Wei,Xuefan Wang, Xia Chen, Chaohao Kan, *Research on Brushless Doubly-Fed Machine with a New Wound Rotor and its Generating System*, Progress on Electromagnetics Research Symposium Proceedings, Moscow, Russia, Aug. 2009, PP.1957-1961.

[4]Paul C. Roberts, *A Study of Brushless Doubly-Fed (Induction) Machines*, PHD Thesis, Emmenuel College, University of Cambridge, 2005.
[5]P. C. Roberts,R. A. McMohan,P. J. Tavner, J. M. Maciejowski, T. J. Flack, *Equivalent Circuit for The Brushless Doubly Fed Machine (BDFM) Including Parameter Estimation and Experimental Verification*, IEE. Proc._Electr. Power Appl., Vol. 152, No. 4, July 2005, PP.933-942.
[6]P. C. Roberts,R. A. McMohan,P. J. Tavner, J. M. Maciejowski, T. J. Flack,X. Wang, *Performance of Rotors in a Brushless Doubly-Fed Induction Machine (BDFM)* , International Conference of Electrical Machines, Maracow, Poland, 2004.
[7]Ruqi Li, *Dynamic Modeling, Simulation and Stability Analysis of Brushless Doubly-Fed Machines*, PHD Thesis, Oregon State University, 1991.
[8] G. Javonovic, *A Comparative Study of Control Strategies for Performance Optimization of Brushless Doubly-Fed Reluctance Machines*, J.Electrical Systems, vol.8, 2006, PP. 208-225.
[9]H. S. EL_SAYED,F. M. EL_KHOULY,A. M. OSHEIBA, *Performance Analysis and Control of a Brushless Doubly Fed Reluctance Machine*, Electric Power Components and Systems, vol.33, 2005, PP.1105-1122.
[10] E. M. Schulz and R. Betz, *Optimal Rotor Design of Brushless Doubly Fed Reluctance Machines*, IEEE Transactions, 2003, PP. 256-261.
[11] R. E. Betz, M. G. Javonovic, *Introduction to the Space Vector Modeling of the Brushless Doubly-Fed Reluctance Machine*, Electric Power Components and Systems, vol.31, Aug. 2003, PP. 729-755.
[12] M. G. Javonovic, R. E. Betz, and J.Yu ,*The Use of Doubly Fed Reluctance Machines for Large Pumps and Wind Turbines*, IEEE Transactions, vol. 3,Dec. 2002, PP. 1508-1516.
[13]Milutin G. Jovanovic, Robert E. Betz, *Control Strategies for Brushless Doubly Fed Reluctance Machines*, T. IEE Japan, vol.121-D, No. 2, 2001, PP.272-278.
[14] R. Betz and M. Gavonovic, *Control Aspects of Brushless Doubly Fed Reluctance Machines*, Proceedings of the European Power Electronics Conference (EPE'99), Sept. 1999.
[15] R. Betz and M. Gavonovic, *Introduction to Brushless Doubly Fed Reluctance Machines- The Basic Equations*, Tech. Rep. EE0023, Department of Electrical Engineering, University of Newcastle, Australia, April 1998.
[16] M El_Shanawany, SMR Tahoun and M Ezzat, *A Dual Stator Winding Brushless Mixed Pole Synchronous Generator "Design, Performance Analysis and Simulation"*, The 10th International Conference on Electric Power System, High Voltage and Electric Machines, Japan, 4-6 Oct. 2010, PP. 159-165.